2020 SCEC Report

Project #20043

# Evaluating the inter-frequency correlation of CyberShake simulations.

Jeff Bayless and Scott Condon
AECOM, Los Angeles

March 12, 2021

With special thanks to Scott Callaghan for his help accessing the CyberShake ground motions.

## Table of Contents

# Abstract

There is increasing recognition that simulations can be utilized in engineering applications, but the simulations require application-specific validation first. In this SCEC study, we evaluate the inter-frequency correlation of Fourier amplitude spectra (FAS) residuals from CyberShake v15.4 simulations, including comparisons with an empirical model.

We collect a database of CyberShake simulations, process the ground motions, perform a residual analysis, and evaluate the inter-frequency correlation of the residuals. Two accomplishments are made towards a broader CyberShake validation. One, we facilitate future validations of inter-frequency correlation by providing a repeatable framework. Second, we find that between 0.1 - 0.5 Hz the simulations have a satisfactory level of total inter-frequency correlation, which is a significant improvement from the conclusions of Bayless and Abrahamson (2018) about the SCEC BBP simulations.

We observe that the between-site component of the residuals has correlation which is significantly higher than the empirical model at frequencies below 0.5 Hz, but is lower at frequencies above 0.5 Hz. This discrepancy may be due to the smoothness of the seismic velocity model in the near surface, or it may be related to the effects of low frequency basin waves mapped into the site terms.

In a future study, we would like to investigate the cause of large correlation for the between-site component of the residuals (by evaluating the effect of low frequency basin waves on the analysis, by utilizing results from alternative GTL models, or by investigating repeatable path effects). Additionally, we would like to repeat our analysis with higher fmax CyberShake simulations (e.g. v15.12) and other regions (e.g. v17.3, v18.8).

# 1. Introduction

Over the past decade-plus, the SCEC CyberShake research project (Graves et al. 2011) has made tremendous progress toward physics-based probabilistic seismic hazard analysis (PSHA). The CyberShake approach uses 3D wave propagation simulations and finite-fault rupture descriptions to forecast ground motions that will be produced by specific ruptures (e.g. the UCERF2 catalog) in California.

There is increasing recognition in the seismological community that simulations, such as those from CyberShake, can be utilized in future engineering applications. But for the simulations to be used in forward applications, they need to be validated first. Validation involves comparing the simulations with observations and with empirical models, e.g., Goulet et al. (2015), Burks (2014), Bayless and Abrahamson (2018a). Validation of the simulations should be carried out for the ground motion parameters relevant to the intended application.

In this SCEC study, we evaluate the inter-frequency correlation of Fourier amplitude spectra (FAS) residuals from CyberShake v15.4 simulations, including comparisons with an empirical model. This procedure contains four components: 1) CyberShake simulation data collection, 2) simulation data processing, 3) residual analysis, and 4) the inter-frequency correlation analysis.

### *1.1 Background*

This study builds upon Jeff Bayless' PhD dissertation, which focused on the validation of ground motion simulation methods on the SCEC Broadband Platform for their inter-frequency correlation. Bayless and Abrahamson (2018a) showed that the appropriate inter-frequency correlations are required to correctly estimate structural seismic fragilities and risk, because the ground motion inter-frequency correlation is related to the width of peaks and troughs in a spectrum (either a Fourier or response spectrum), and the structural response variability can be under-estimated if the inter-frequency correlation is too low. Low structural response variability leads to fragility curves that are too steep, and to un-conservative estimates of seismic risk (Bayless and Abrahamson, 2018a). These conclusions apply to structural risk assessments derived from ground motion simulations, commonly referred to as "ruptures to rafters" simulations.

In Bayless and Abrahamson (2018a) the authors evaluated six SCEC BBP simulation methods and compared the inter-frequency correlations with the Bayless and Abrahamson (2018b; BA18Corr hereafter) empirical model developed from the NGA-W2 database (Ancheta et al. 2014) ground motions. Bayless and Abrahamson (2018a) found that none of the six tested finite-fault simulation methods adequately captured the correlations over the entire frequency range evaluated, and although several of the methods showed promise at low frequencies, the total correlations were low compared with BA18Corr.

However, the Bayless and Abrahamson (2018a) conclusions were partly blurred by procedural differences in the residual analyses performed on the simulations and on the NGA-W2 data. The SCEC BBP simulation methods generally use 1-D Green's functions for the low frequency part of the simulations, and because of this, the residual analysis was tailored to the ground motion simulations available, which led to the following differences:

- The simulations are based on plane-layered (1-D) seismic velocity models so all sites for a given scenario have the same shear wave velocity at the surface, and there is no variability in the site response. Therefore the "site terms" in the 1-D simulations do not have the same meaning as they do in a residual analysis from a recorded database like NGA-W2, where each site has a unique velocity profile beneath it with characteristic

effects. In Bayless and Abrahamson (2018a) the site term could not be distinguished from the constant term.

- The “source terms” in the BBP simulations were determined from alternative realizations of the same earthquakes with different slip distributions, whereas in the NGA-W2 database each earthquake has unique properties (such as location, dimensions, slip, and hypocenter, etc).

By using CyberShake v15.4 in this study, and by selecting a wide range of sources, sites, and site conditions, we better mimic the distribution of data in the NGA-W2 database (on which the empirical correlation model is based.) This allows for separation of the FAS residuals into repeatable source, repeatable site, and remainder components. This greatly simplifies the comparison between inter-frequency correlations calculated for the CyberShake ground motions and from NGA-W2.

In the remainder of this report, we describe the subset of the CyberShake database we have collected and processed (Section 2), our FAS residual analysis (Section 3), the inter-frequency correlation analysis (Section 5), and conclusions (Section 6).

# 2. Database

### *2.1 Cybershake Version Information*

CyberShake is a computational study to calculate ground motion hazard in the Los Angeles region (Graves et al., 2011). Others have used CyberShake for ground motion studies and simulation validation, e.g. Chen and Baker, 2019; Wang and Jordan, 2014; Villani and Abrahamson, 2015. CyberShake v15.4 includes simulations of over 415,000 UCERF2 rupture realizations at 336 sites and simulates wave propagation through a three-dimensional velocity model that reflects the impact of sedimentary basins and near-surface materials on ground motion (Chen and Baker, 2019). Figure 1 shows a map of the CyberShake v15.4 region and sites, color-coded by the 2-second spectral acceleration hazard with 2% probability of exceedance in 50 years.

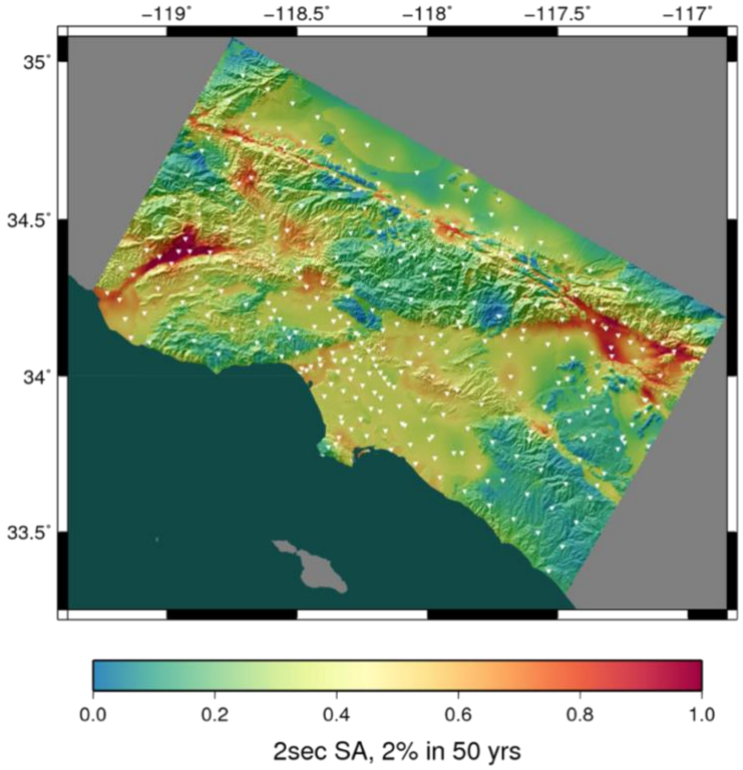


**Figure 1.** A map of the CyberShake v15.4 domain, with site locations indicated by white triangles. Figure source: https://strike.scec.org/scecpedia/CyberShake_Study_15.4

CyberShake v15.4 is a low-frequency study (f<1 Hz) using the UCERF2 (Field et al., 2009) kinematic sources with the Graves and Pitarka (2015) rupture generator. With the sources defined, CyberShake uses an elastic wave propagation simulation to calculate Strain Green tensors around the site of interest, and seismic reciprocity is used to obtain synthetic seismograms (Graves et al., 2011). The 3-D seismic velocity model used is the CVM-S4.26.M01; this is the tomography improved southern CA model with a 500m resolution, is tri-linearly interpolated, and has minimum Vs of 500 m/s (Small et al., 2017). The 'M01' in this velocity model version name refers to the algorithm used to modify the near-surface material properties (called the geotechnical layer, or GTL). The M01 GTL was derived to put back the original GTL of CVM-S4 (Magistrale et al., 2000) into the raw CVM-S4.26 model (Taborda et al., 2016).

The purpose of the GTL model is to emulate the presence of weathered rocks and deposits in the upper few hundred meters and provide a transition to the stiffer bedrock basement of the underlying CVM-S4.26 model (Small et al., 2017). In the CVM-S4.26.M01, the GTL was implemented by Ricardo Taborda and is based on rock/soil profiles from Walt Silva as implemented by Magistrale et al., (2000) (Rob Graves, personal communication).

Because the GTL (upper 350m) of the seismic velocity model is based on averages of geotechnical profiles smoothed and interpolated to larger areas (Magistrale et al., 2000), the CVM in the near surface is quite generic and does not have the detailed irregularities of real velocity profiles. Additionally, due to the averaging and interpolation, the variability in the GTL profiles is lower than reality. This has important implications for the inter-frequency correlations we calculate in Section 4.

### *2.2 Cybershake Data Selection and Acquisition*

The selection and acquisition of CyberShake simulations and metadata can be separated into four parts: (1) event selection, (2) metadata acquisition, (3) waveform acquisition, and (4) data compilation. The procedure outline below can be followed using the tools made available at github.com/scndn/cybershake and necessitates a basic knowledge of programming and access to the intensity@usc.edu server.

In (1) event selection, we query the CyberShake SQL database for all simulated ground motions belonging to Study 15.4 and return a subset of unique simulation identification integers (IDs).

In (2) metadata acquisition, we use the subset of simulation IDs from step (1) to query the CyberShake SQL database for all relevant metadata related to the earthquake source and recording station. This information includes source magnitude, source hypocenter, station location, $Vs_{30}$, $Z_{1.0}$, and $Z_{2.5}$.

In (3) waveform acquisition, we use the subset of simulation IDs from step (1) to download simulated waveforms and earthquake source rupture files stored on intensity@usc.edu. Each earthquake source rupture file contains a grid of point sources defined by latitude, longitude, depth, rake, dip, and strike.

In (4) data compilation, we compile existing and compute additional metadata using the earthquake source rupture files and process the simulated waveforms using scripts made available on intensity@usc.edu. We compute Rrup using the site location and earthquake rupture discretization, $Z_{tor}$ using the earthquake source rupture file, and rake angle as the weighted average rake of the rupture discretization.

The final database of selected CyberShake v15.4 acceleration time histories and metadata include the following metadata for each simulated ground motion: Run_ID, Source_ID, Rupture_ID, Rupture_Variation_ID, earthquake source name, earthquake magnitude, Site_ID, site name, Rrup, $Vs_{30}$, $Z_{tor}$, $Z_{1.0}$, $Z_{2.5}$, rake, and accompanying acceleration time histories.

### *3.3 Selected Subset*

Using the selection procedure described above, we have compiled a database of CyberShake v15.4 acceleration time histories and metadata. The database consists of the 336 unique CyberShake stations from 188 UCERF2 earthquake scenarios spanning **M**6.25 – **M**7.95. For each earthquake source, we randomly select one of the available rupture realizations. For each earthquake we select approximately 26 stations with rupture distances ranging from 0-200 km. This results in 4,904 two-component acceleration time histories. We select sites with Vs30 < 1,500 m/s to approximately match the bulk of the NGA-W2 data. Figure 2 shows a map of the simulation stations and earthquake hypocenters in this data subset.

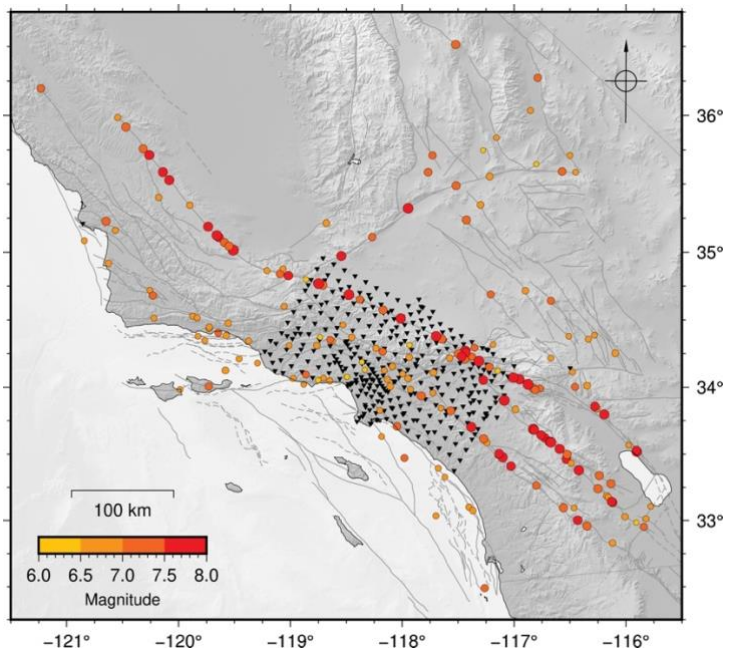


**Figure 2.** A map of the subset of CyberShake v15.4 sites (triangles) and sources (circles) used in this study.

Figure 3 shows, for the two databases, **M** vs distance scatterplots of the data and histograms of parameters **M**, Ztor, Rrup, Vs30, and Z1.0. The CyberShake database is shown in (a) and the NGA-W2 database used to develop BA18Corr is shown in (b). Overall, we achieve the goal of creating a CyberShake database that has a distribution of earthquake magnitudes, site distances, and site conditions that is comparable to a recorded database like the NGA-W2. The minimum **M** in CyberShake is notably larger than the smallest **M** from the NGA-W2 database, however this is not expected to be a problem because Bayless and Abrahamson (2018b) did not find any statistically significant dependence of the inter-frequency correlation on **M**. The range of rupture distances in the CyberShake database matches the NGA-W2 well, although in a future iteration of our selection scripts we may include a preference for smaller Rrup to better match the NGA-W2 data. For most events, there are more stations available at regional distances because many of the earthquakes occur away from the grid of CyberShake stations (Figure 2).

The most important difference between our CyberShake database and the NGA-W2 is in the site conditions. The CyberShake v15.4 Vs30 values are from the CVM 3-D mesh. Many of the sites have a Vs30 of 500 m/s because SCEC used a Vs floor of 500 m/s in the CyberShake velocity meshes, so all the basin low-velocity sites end up with Vs30=500 m/s (Scott Callaghan, personal communication). The minimum Vs30 of 500 m/s is a much higher floor value than in the NGA database, which has Vs30 as low as 150 m/s. Vs30 = 500 m/s is also slightly higher than the modal bin of the NGA-W2 Vs30's as shown in Figure 3. The small variability in GTL profiles (and in Vs30) inflates the inter-frequency correlation of the CyberShake between-site residuals, as discussed in Section 4.

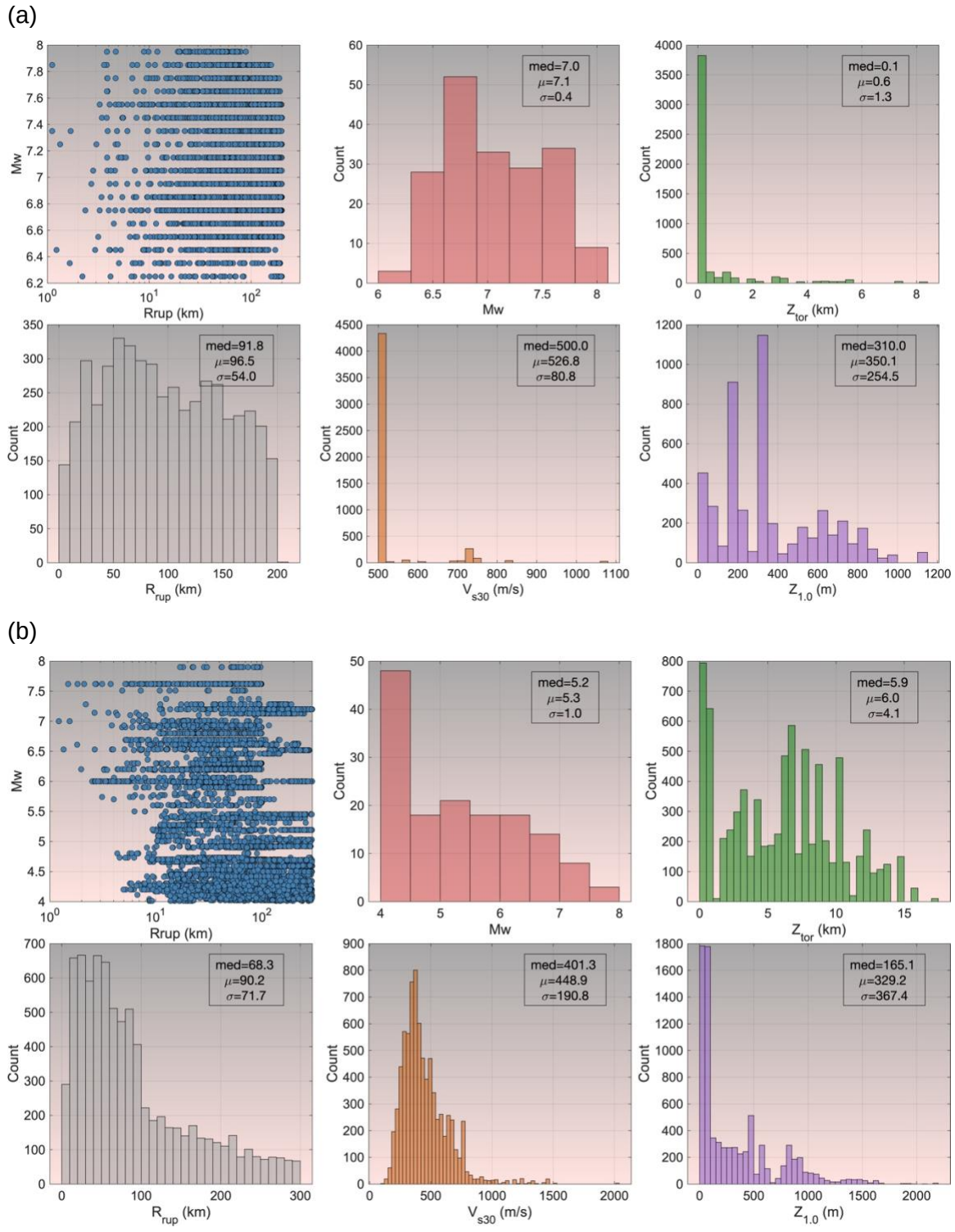


**Figure 3.** Distributions of various parameters in the CyberShake database used in this study (a) and in the subset of the NGA-W2 database (b) used to develop BA18Corr.

### *3.3 Simulation Data Processing*

From the simulated acceleration time series, we calculate the FAS for both horizontal components, the Effective Amplitude Spectra (EAS; Goulet et al., 2018), and the smoothed EAS, following the procedure established by NGA-East (PEER, 2015) and described in Bayless and Abrahamson (2019; BA19 hereafter). The BA19 empirical ground motion model we use for calculating residuals (described in Section 3) is valid over frequencies 0.1 – 24 Hz, and the CyberShake v15.4 simulations are valid for f < 1.0 Hz, therefore our analysis is for the range 0.1 – 1.0 Hz. A flatfile of the smoothed EAS and metadata is provided in the Appendix of this report.

In Figure 4, an example of these products is shown for one synthetic ground motion. As shown in Figure 4, we calculate the FAS for frequencies up to the Nyquist, although in subsequent steps the FAS is only used up to the maximum frequency of the simulations, 1 Hz.

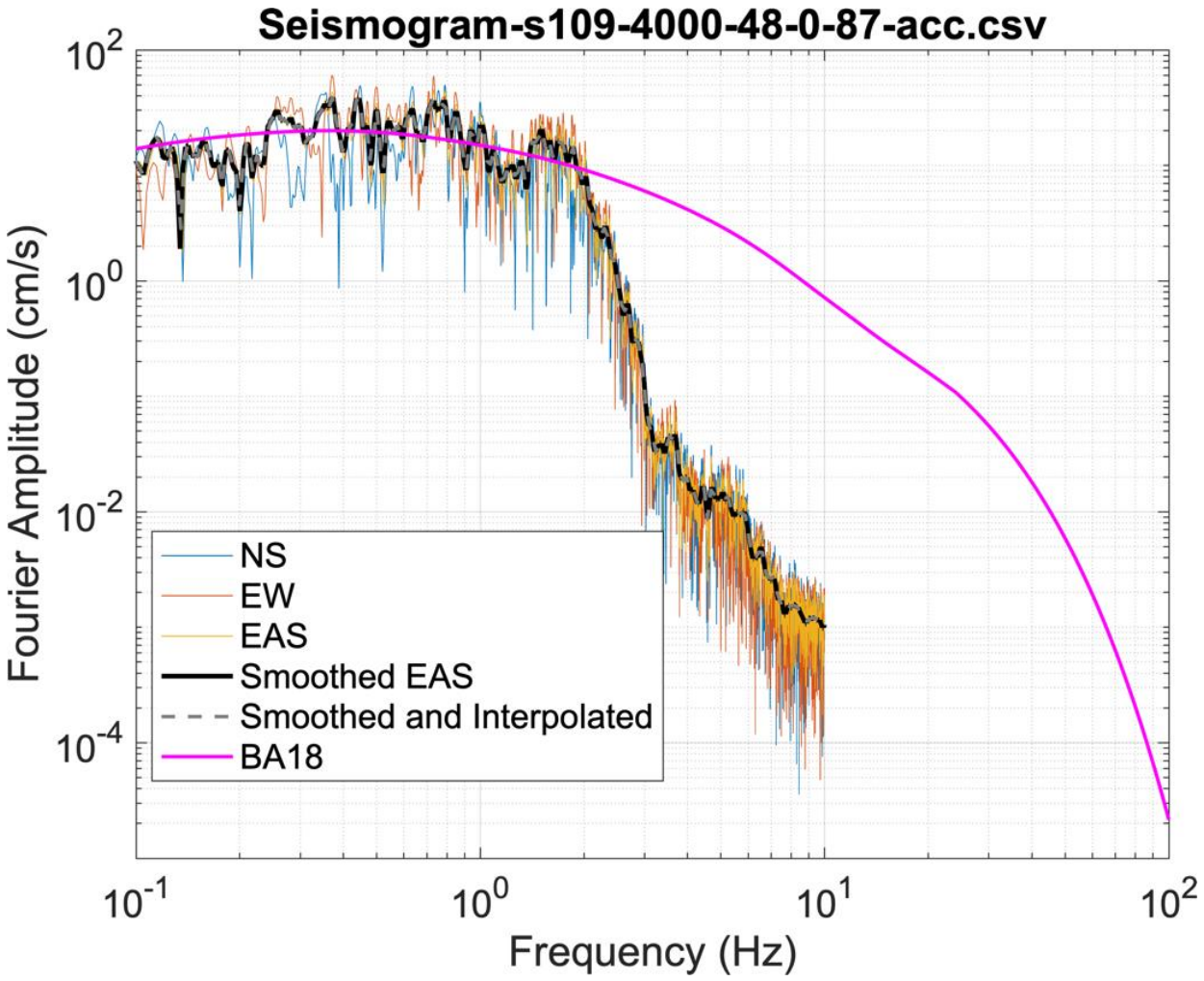


**Figure 4.** The NS and EW component FAS, orientation independent EAS, smoothed EAS, EAS interpolated to the frequencies used in the residual analysis, and the median Bayless and Abrahamson (2019) model EAS prediction for an example CyberShake ground motion. In this example, good agreement is shown between the CyberShake EAS and the BA19 median prediction, for f<1 Hz, which is the usable range of the simulation.

# 3. Residual Analysis

Using the BA19 EAS ground motion model for California, we calculate EAS residuals for our CyberShake database. Following Villani and Abrahamson (2015) and Bayless and Abrahamson (2018a), the residuals take the form of Equation 1:

$$\delta_{total}(f) = Y(f) - g(X_{es}, \theta, f) = \delta B_e(f) + \delta S2S_s(f) + \delta WS_{es} + C(f) \quad (1)$$

where $Y(f)$ is the natural log of the CyberShake smoothed EAS at frequency $f$, $g(X_{es}, \theta, f)$ is the median BA19 GMM, $X_{es}$ is the vector of explanatory seismological parameters (magnitude, distance, site conditions, etc.), $\theta(f)$ is the vector of GMM coefficients, and $\delta_{total}(f)$ is the total residual for earthquake $e$ and site $s$. The residual components $\delta B_e(f)$, $\delta S2S_s(f)$, and $\delta WS_{es}(f)$ represent the between-event, site-to-site, and single station within-site residuals, respectively. $C(f)$ represents the mean total residual, or the mean bias. The mean bias exists because the median EAS from the simulations is different from the empirical model for a given scenario. We remove the overall bias between the simulations and the empirical model by removing $C(f)$ (Figure 5). The cause of the mean bias is a topic for a future study.

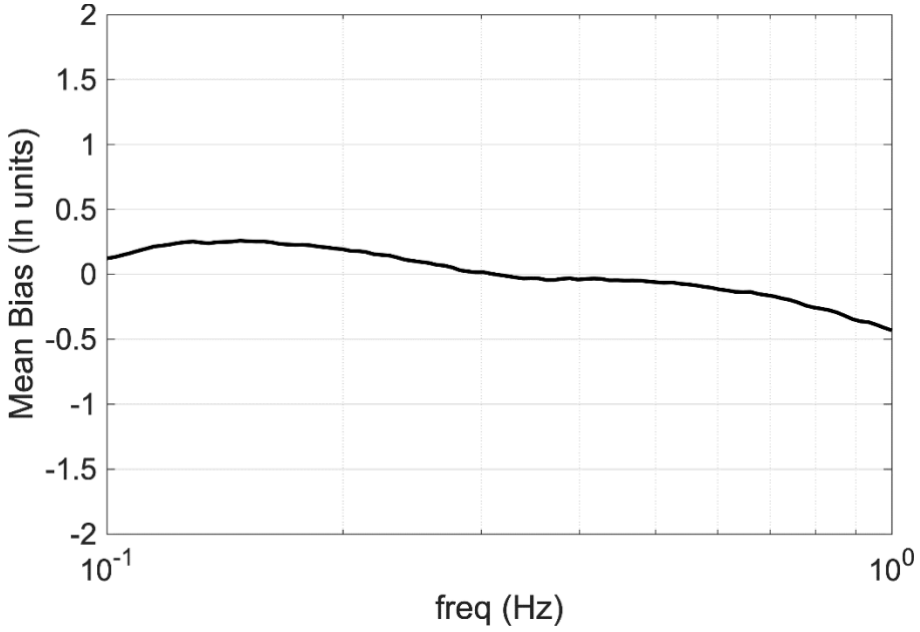


**Figure 5.** The frequency dependence of the mean bias term, $\boldsymbol{C}$.

Once we have removed the mean bias from the residuals, the event terms ($\delta B_e(f)$, specific to each earthquake) and ($\delta S2S_s(f)$, specific to each site) are calculated and removed using a mixed effects regression. Histograms of the event and site terms, for all frequencies analyzed, are shown in Figure 6. The residual components $\delta B_e$, $\delta S2S_s$, and $\delta WS_{es}$ are well represented as zero mean, independent, normally distributed random variables with standard deviations $\tau$, $\phi_{S2S}$, and $\phi_{SS}$, respectively.

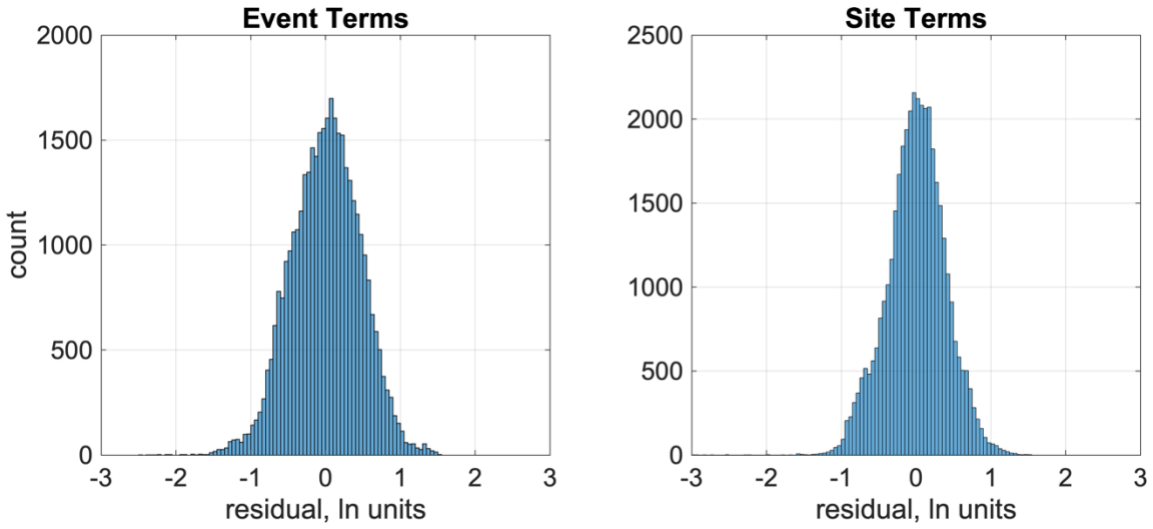


**Figure 6.** Histograms of event terms and site terms from the residual analysis.

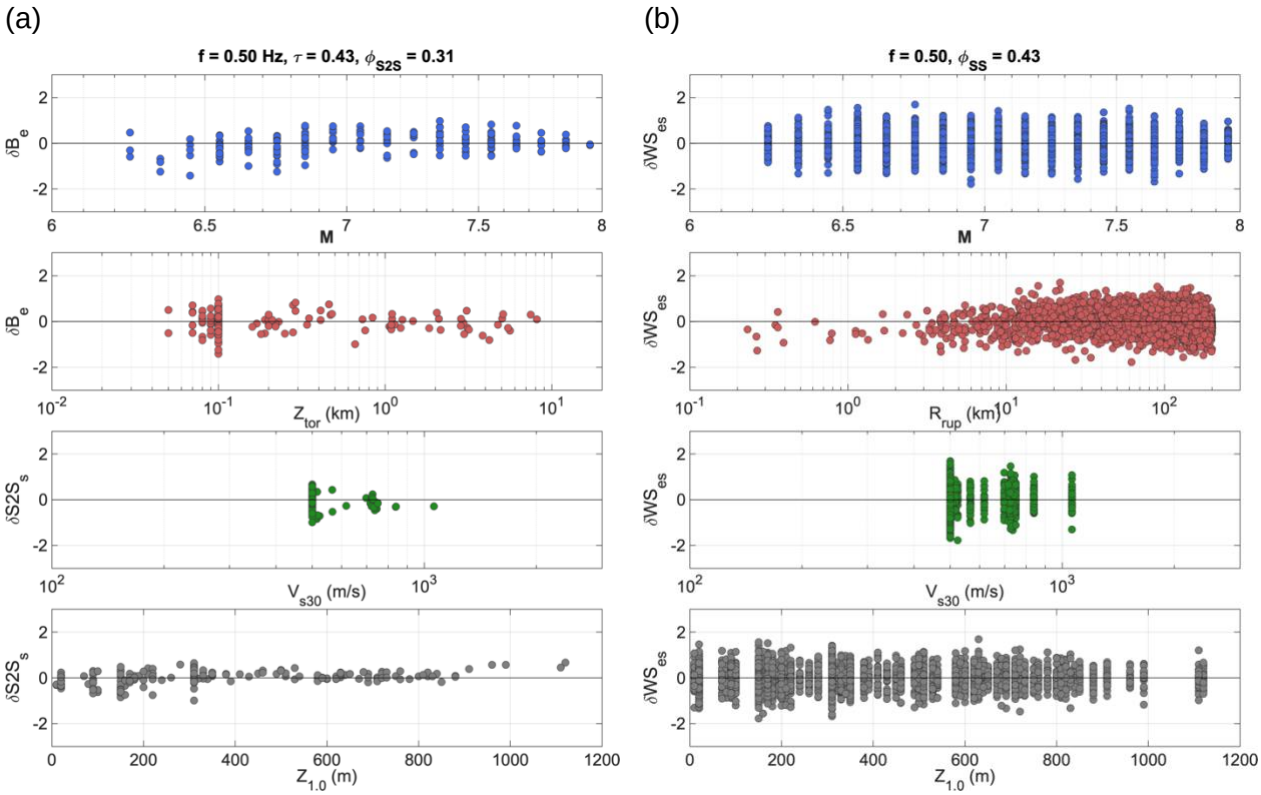


**Figure 7.** CyberShake EAS residuals at f=0.5 Hz versus various predictor variables. (a) Event and Site terms. (b) Within-site residuals.

We evaluate the residuals from the regression analysis as functions of the main model parameters in order to check for errors or strong trends. The presence of obvious strong trends in the residuals versus predictor variables would indicate that the simulations do not agree with that component of the reference model. In Figure 7, we show an example of this residual analysis at f=0.5 Hz. In the left column, the event and site terms are evaluated versus **M**, depth to the top of the rupture plane (Ztor), Vs30, and Z1.0. In the right column, the within-site residuals are evaluated versus **M**, Rrup, Vs30, and Z1.0. There are no apparent trends in the within-site residuals at f=5 Hz. At left, the event terms potentially show a weak magnitude dependence; for **M**<6.5 the event terms are biased low, which indicates that the BA19 median model over predicts the ground motions from the simulated earthquakes in this range, on average. The event terms do not exhibit strong trends with Ztor. The site terms do not show strong trends with Vs30, although the range of available Vs30 values is less than ideal, as discussed previously. Finally, the site terms do not show strong trends with basin depth parameter Z1.0, although the site-term residuals tend to be positive for Z1.0 greater than about 1km, indicating that the scaling for deeper basin sites is slightly stronger in the simulations than in BA19.

We believe these residuals, and the similar results at other frequencies in the range 0.1 – 1.0 Hz, are suitable for the purposes of calculating the inter-frequency correlation in the next section. Several interesting observations, such as the **M**-scaling and mean bias, are excellent topics for a future study.

Figure 8(a) shows the frequency dependence of the standard deviations of each residual component, along with the total standard deviation ($\sigma$). Figure 8(b) is replicated from Bayless and Abrahamson (2018b; their Figure 3) and shows the same standard deviation components calculated from the NGA-W2 data. Our event term standard deviation, $\tau$, is largest at frequencies less than about 0.3 Hz, and has a peak value of about 0.6 natural log units, which is broadly consistent with (b). At about 1 Hz, our site term standard deviation, $\phi_{S2S}$, is significantly lower than in (b). Our within-site variability, $\phi_{SS}$, varies between about 0.4 and 0.5 natural log units, which is also broadly consistent with (b).

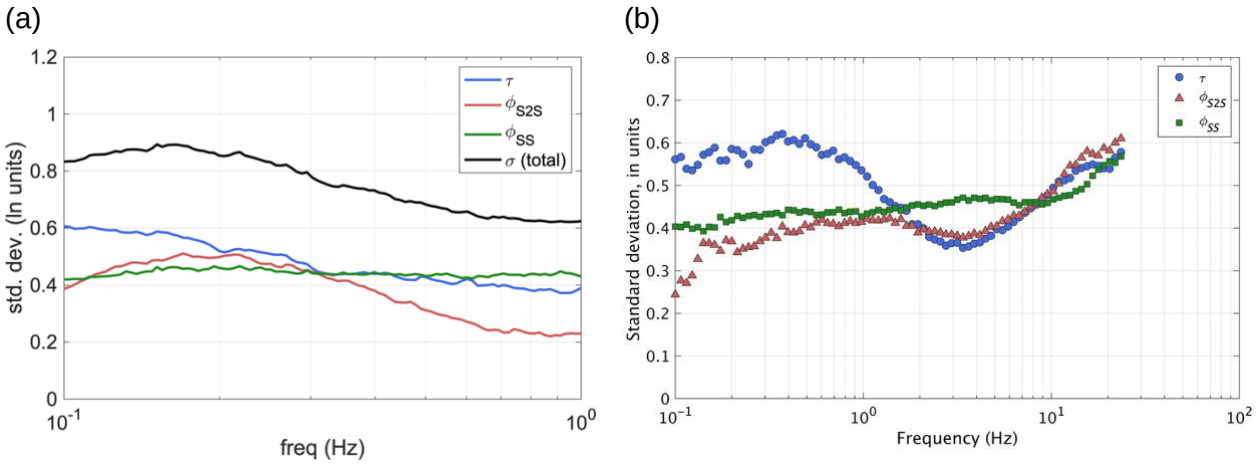


**Figure 8.** Frequency dependence of the standard deviations of the residual components from (a) this study and (b) BA18Corr

# 4. Inter-frequency Correlations

The EAS residual components are converted to epsilon ($\epsilon$) by normalizing the residuals by their respective standard deviations:

$$\epsilon_B(f) = \frac{\delta B_e(f)}{\tau(f)}$$
$$\epsilon_{S2S}(f) = \frac{\delta S2S_s(f)}{\phi_{S2S}(f)} \quad (2)$$
$$\epsilon_{WS}(f) = \frac{\delta WS_{es}(f)}{\phi_{SS}(f)}$$

Because of the normalization, the random variables $\epsilon_B$, $\epsilon_{S2S}$, and $\epsilon_{WS}$ are well-represented by standard normal distributions (mean = 0 and variance = 1). We calculate the inter-frequency Pearson-product-moment correlation coefficient ($\rho$; Fisher, 1958) of each $\epsilon$ component ($\rho_{\epsilon,EAS}$), as well as the total correlation using Equations 3 and 4 of Bayless and Abrahamson, 2018b. All correlations presented in this report are for the smoothed EAS, and for notational brevity the EAS subscript is dropped hereafter. Similarly, if not stated explicitly, the term "inter-frequency" is implied in all uses of the word "correlation" in this report because this is the only type of correlation we evaluate.

The $\rho_\epsilon$ calculation can be repeated for every frequency pair of interest and the resulting correlation coefficients for each pair of frequencies can be saved as tables and displayed as contours. Figure 9 shows contours of the total $\rho_\epsilon$ for (a) this CyberShake study and (b) Bayless and Abrahamson, 2018b. Both panels of this figure have the same color scale, and the horizontal and vertical axes are frequencies ranging from 0.01 – 1.0 Hz. These figures are symmetric about the 1:1 line because the correlation coefficient between two frequencies is the same regardless of which frequency is the conditioning frequency.

(a) (b)

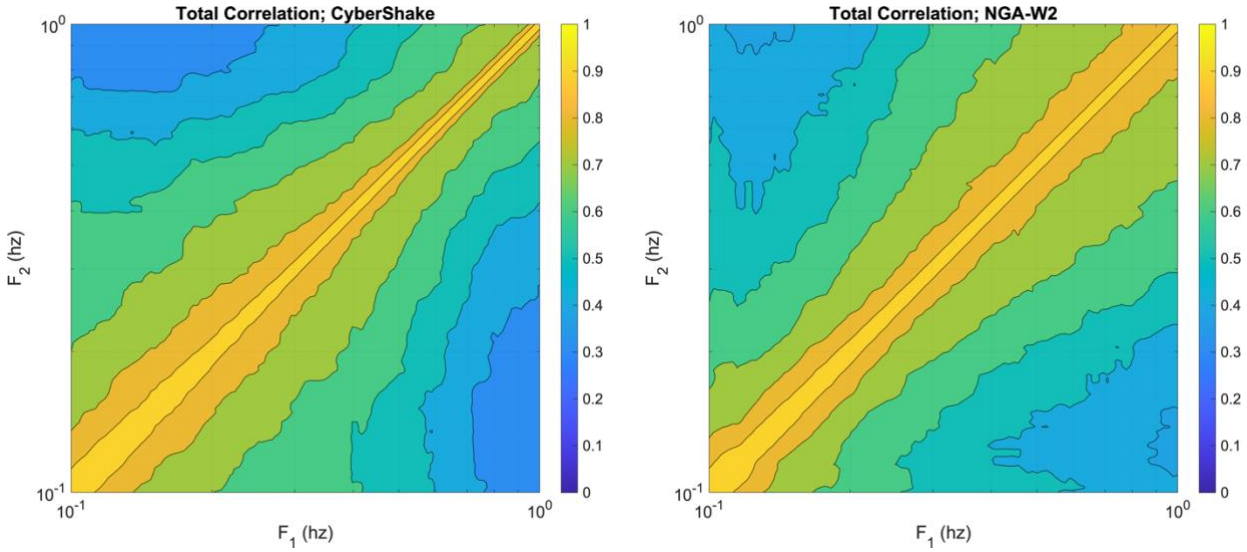


**Figure 9.** Contours of total $\boldsymbol{\rho_\epsilon}$ for (a) this CyberShake study and (b) BA18Corr (Bayless and Abrahamson, 2018b).

The total $\rho_\epsilon$ contours in Figure 9 are helpful for making large-scale comparisons. In this sense, the correlation from the CyberShake residuals look quite good compared with BA18Corr.

Previously, Bayless and Abrahamson (2018a) evaluated six different simulation methods on the SCEC BBP, and their conclusions varied by method, but they found generally poor match at frequencies greater than about 0.5 Hz, and too rapid a decay of the correlation at frequencies away from the conditioning frequency. The result shown here is a noticeable improvement.

To qualitatively analyze these results, it is helpful to deconstruct the $\rho_\epsilon$ contours into cross sections at select conditioning frequencies; this is equivalent to taking "slices" of the contours. In Figure 10, we show the total $\rho_\epsilon$ cross section at conditioning frequency 0.15 Hz. In this figure, solid line is the total $\rho_\epsilon$ from this study, and the dashed line is from BA18Corr. The darker and lighter shaded regions represent the 95% confidence intervals of $\rho_\epsilon$ from these studies respectively (Kutner et al, 2005). When the 95% confidence intervals don't overlap, there is a statistically significant difference between the $\rho_\epsilon$ (at the 0.05 level of significance). For most frequencies in Figure 10, these confidence intervals overlap, even if only slightly.

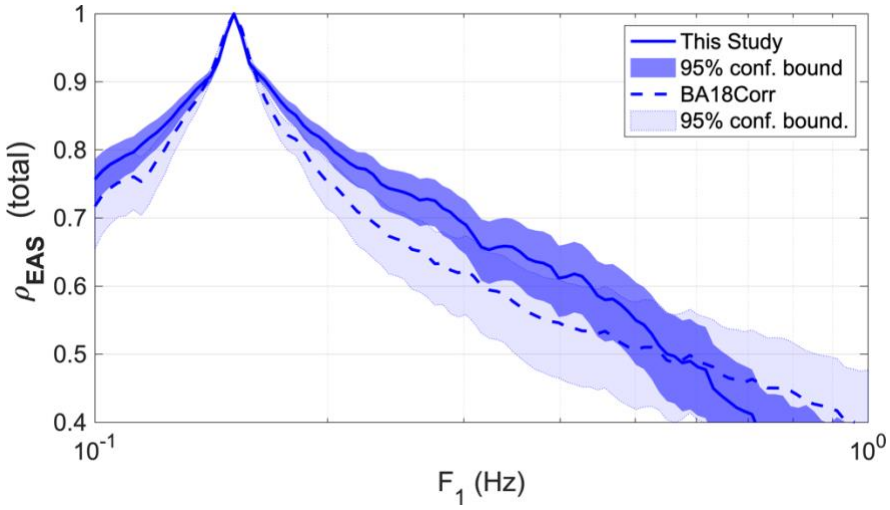


**Figure 10.** Total $\boldsymbol{\rho_\epsilon}$ cross sections at conditioning frequency 0.15 Hz. The results from this study are shown by the solid heavy line, with 95% confidence bound shown by the heavy fill. The results from BA18Corr are shown by the dashed line, with light fill representing the 95% confidence bounds.

In Figure 11, $\rho_\epsilon$ cross sections are shown at conditioning frequencies 0.15, 0.33, and 1.0 Hz. To increase readability, we only show the 95% confidence bounds on $\rho_\epsilon$. Panels (a) through (d) show the $\rho_\epsilon$ cross sections for the event terms, site terms, within-site terms, and the total correlation. As in Figure 10, the darker fill corresponds to this study, and the lighter, transparent fill corresponds to BA18Corr. Each panel of this figure is discussed in the following paragraphs.

In Figure 11(a), the between-event $\rho_\epsilon$ cross sections are compared. Out of the three residuals components, these have the widest confidence intervals because there are the fewest samples of the between-event terms (earthquakes) for calculating $\rho_\epsilon$. The between-event $\rho_\epsilon$ physically relates to source effects (e.g. stress drop), which drive ground motions over a broad frequency range and thus lead to relatively broad $\rho_\epsilon$ (Bayless and Abrahamson, 2018a). At frequencies less than about 0.5 Hz, the 95% confidence bands from this study match BA18Corr very well. At frequencies between 0.5 and 1.0 Hz, the 95% confidence bands do not overlap and the CyberShake $\rho_\epsilon$ are much lower than BA18Corr. The match deteriorates as frequencies increase towards the upper limit of the simulations; this may be related to the resolution of the seismic velocity model. In the future, we would like to test this idea by repeating our validation exercise using the more recent CyberShake runs which feature improved seismic velocity models (e.g. SCEC CVM-S4.26.M01; Small et al., 2017).

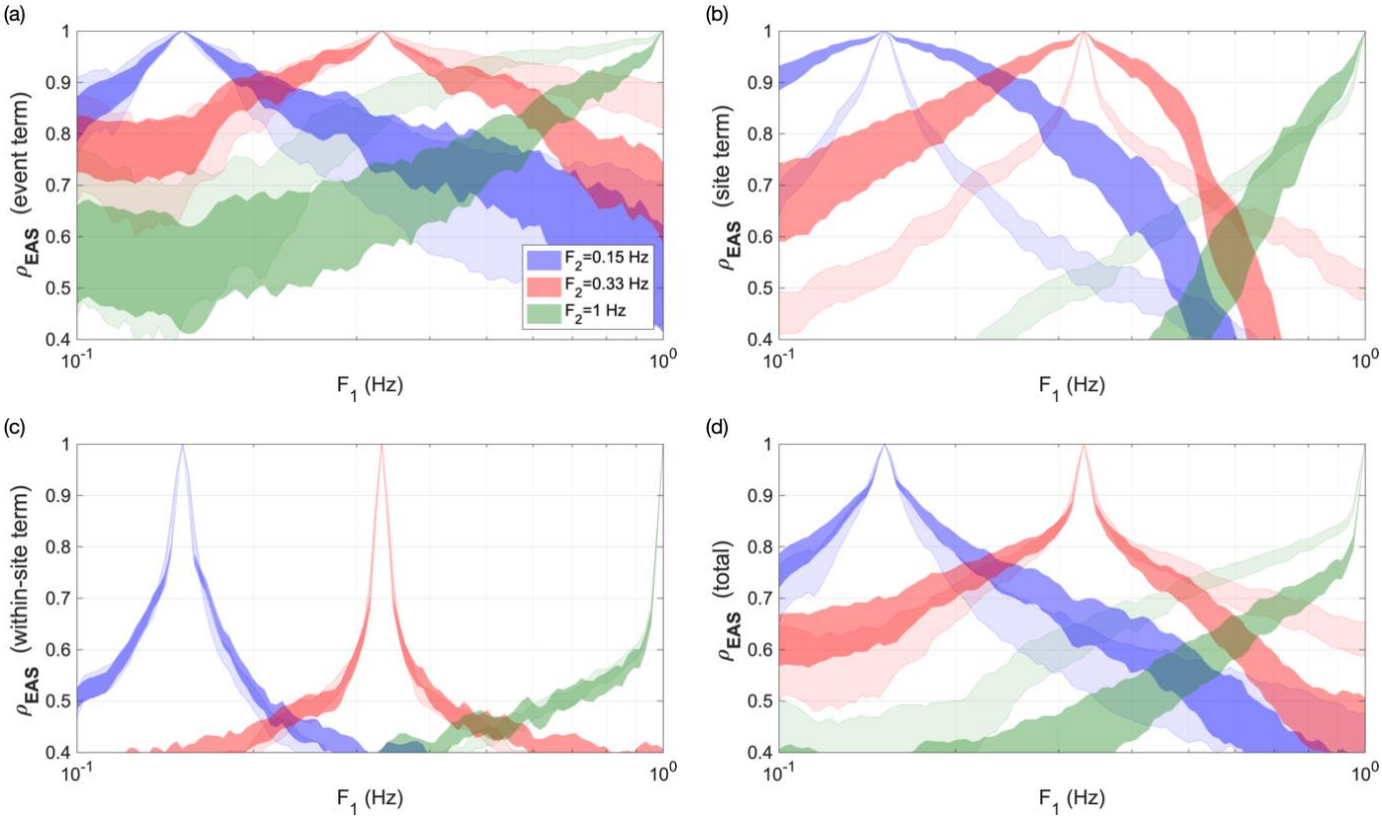


**Figure 11.** Cross sections of $\boldsymbol{\rho_\epsilon}$ 95% confidence bounds at three conditioning frequencies. The darker fill corresponds to this study, and the lighter fill corresponds to BA18Corr. For (a) the between-event component, (b) the site-to-site component, (c) the within-site component, and (d) the total correlation.

In Figure 11(b), the site-to-site $\rho_\epsilon$ cross sections are compared. The between-site residual represents the systematic deviation of the observed amplification at a site from the median amplification predicted by the model. Therefore, the site-to-site $\rho_\epsilon$ represents the inter-frequency correlation of the systematic site amplification deviations. Of the three residual components, we find the largest difference in $\rho_\epsilon$ between this study and BA18Corr, with generally larger correlation at frequencies less than about 0.5 Hz, and lower correlation for the higher frequencies (a similar trend to the between-event correlations). The larger site-to-site $\rho_\epsilon$ below 0.5 Hz propagates through to the total $\rho_\epsilon$ in panel (d). This effect is likely related to the way in which CyberShake v15.4 (using CVM-S4.26.M01) has modeled the near surface, or GTL. As mentioned previously, the GTL is based on averaged and spatially smoothed geotechnical profiles from borehole measurements (Magistrale et al., 2000). Since the GTL is based on average profiles, the site amplification from the simulations will represent these average profiles and will feature broad frequency bands of amplification. Conversely, in a database of recorded ground motions, the between-site residual represents the characteristic amplification at the site due to amplification of the seismic waves produced by variations of the material properties in these layers. These characteristic amplifications will be peaked over frequency bands which correspond to the resonant frequencies of the profiles.

Another potential source of the mismatch observed in Figure 11(b) is the effect of low frequency basin waves. These are surface waves usually produced by the conversion of body waves at the edge of basin into surface waves that propagate across the basin and have very long periods. The basin depth parameter (Z1.0) scaling is meant to capture these effects in an

average sense, but if these effects are systematic they could be mapped into the site terms and impact the low frequency $\rho_\epsilon$.

In Figure 11(c), the within-site $\rho_\epsilon$ cross sections are compared. The within-site residual component represents the remaining residual after partitioning the random effects for the event and the site. These cross sections are characterized by a steep decay at frequencies very close to the conditioning frequency followed by a relatively flat slope at frequencies farther away from the conditioning frequency. There is generally less inter-frequency correlation from this component of the residuals. In Figure 11(c), the similarity between this study and BA18Corr is excellent. This strong match between the simulations and the recorded data is valuable because, unlike the source- and site- term components of the correlation, it is less clear how one would go about calibrating the within-site $\rho_\epsilon$ in the CyberShake simulations.

Finally, in Figure 11(d), the total $\rho_\epsilon$ cross sections are compared. The total $\rho_\epsilon$ is calculated from Equation 4 of Bayless and Abrahamson, 2018b; it is the combination of all the component $\rho_\epsilon$ weighted by their respective variances. It follows that the total $\rho_\epsilon$ exhibits similar trends as with the other components; with generally larger, satisfactory correlation at frequencies less than about 0.5 Hz, and with lower, less agreeable correlation at higher frequencies.

# 5. Conclusions

As indicated in the Introduction, there is increasing recognition that simulations can be utilized in engineering applications, but the simulations require application-specific validation first. If ground motion simulations are used in seismic fragility and seismic risk analyses, Bayless and Abrahamson (2018a) show that the correlation of normalized residuals (parameter $\epsilon$) is an essential component of the ground motion simulations for capturing the variability of structural response, and therefore should be validated thoroughly.

This study features two accomplishments towards a broader CyberShake validation. One, we facilitate future validations of the simulations against recorded ground motions by providing a framework for evaluating CyberShake inter-frequency correlations. The outline of this study can be repeated using different and more advanced versions of CyberShake, or any other simulation platform, in the future. Second, we find that the $0.1 < f < 0.5$ Hz CyberShake 15.4 simulations have a satisfactory level of inter-frequency correlation, which is a significant improvement from the conclusions of Bayless and Abrahamson (2018a) about the SCEC BBP simulations.

We observe that the between-site component of the residuals has correlation $\rho_\epsilon$ which is significantly higher than the empirical model at frequencies below 0.5 Hz, but has lower $\rho_\epsilon$ than the empirical model at frequencies above 0.5 Hz. This may be due to the relative simplicity of the seismic velocity model in the GTL, or it may be related to the effects of low frequency basin waves mapped into the site terms.

In a future study, we would like to investigate the cause of large correlation $\rho_\epsilon$ for the between-site component of the residuals (by evaluating the effect of low frequency basin waves on the analysis, or by utilizing results from alternative GTL models). We would also like to investigate the presence of repeatable path and basin effects through an in-depth residual analysis. Additionally, we would like to repeat our analysis with higher fmax CyberShake simulations (e.g. v15.12) and for simulations of other regions (e.g. v17.3, v18.8).

# 6. References

Ancheta, TD, RB Darragh, JP Stewart, E Seyhan, WJ Silva, BS-J Chiou, KE Wooddell, RW Graves, AR Kottke, DM Boore, T Kishida, and JL Donahue (2014). NGA-West2 database, *Earthquake Spectra*, **30**, 989-1005.

Bayless, J., and N. A. Abrahamson (2018a). Evaluation of the inter-period correlation of ground motion simulations, Bull. Seismol. Soc. Am. 108, no. 6, 3413–3430, doi: 10.1785/0120180095.

Bayless, J., and N. A. Abrahamson (2018b). An empirical model for the interfrequency correlation of epsilon for Fourier amplitude spectra, Bull. Seismol. Soc. Am. 109, no. 3, 1058–1070, doi: 10.1785/0120180238.

Bayless J, and Abrahamson N.A. (2019) Summary of the BA18 Ground-Motion Model for Fourier Amplitude Spectra for Crustal Earthquakes in California, Bull. Seismol. Soc. Am., 109 (5): 2088-2105. doi: 10.1785/0120180238.

Bozorgnia, Y, NA Abrahamson, L Al Atik, TD Ancheta, GM Atkinson, JW Baker, A Baltay, DM Boore, KW Campbell, BS-J Chiou, R Darragh, S Day, J Donahue, RW Graves, N Gregor, T Hanks, IM Idriss, R Kamai, T Kishida, A Kottke, SA Mahin, S Rezaeian, B Rowshandel, E Seyhan, S Shahi, T Shantz, W Silva, P Spudich, JP Stewart, J Watson-Lamprey, K Wooddell, and R Youngs, 2014. NGA-West 2 research project, *Earthquake Spectra*, **30**, 973-987.

Chen, Y., and Baker, J. W. (2019). “Spatial correlations in CyberShake physics-based ground motion simulations.” Bulletin of the Seismological Society of America, (in press).

Ely, G., T. H. Jordan, P. Small, and P. J. Maechling (2010), A VS30-derived near-surface seismic velocity model, Abstract S51A-1907 presented at 2010 Fall Meeting, AGU, San Francisco, Calif., 13-17 Dec.

Field, E. & Dawson, T. & Felzer, K. & Frankel, A. & Gupta, Vasu & Jordan, Thomas & Parsons, Tom & Petersen, Mark & Stein, R. & Weldon, Ray & Wills, Christopher. (2009). Uniform California Earthquake Rupture Forecast, Version 2 (UCERF 2). Bulletin of The Seismological Society of America. 99. 10.1785/0120080049.

Fisher, R. A. (1958). Statistical Methods for Research Workers, 13th Ed., Hafner, Edinburgh, London.

Goulet, CA, NA Abrahamson, PG Somerville, and KE Wooddell, 2015. The SCEC Broadband Platform validation exercise: Methodology for code validation in the context of seismic hazard analyses, *Seismol. Res. Lett*. **86**, 17-26.

Goulet, C. A., A. Kottke, D. M. Boore, Y. Bozorgnia, J. Hollenback, T. Kishida, A. Der Kiureghian, O. J. Ktenidou, N. M. Kuehn, E. M. Rathje, et al. (2018). Effective amplitude spectrum (EAS) as a metric for ground motion modeling using Fourier amplitudes, 2018 Seismology of the Americas Meeting, Miami, Florida, 14–17 May 2018.

Graves, R., Jordan, T. H., Callaghan, S., Deelman, E., Field, E. H., Juve, G., Kesselman, C., Maechling, P., Mehta, G., Okaya, D., Small, P., Vahi, K. (2011), CyberShake: A Physics-Based Seismic Hazard Model for Southern California, Pure and Applied Geophysics, 168(3-4), 367–381.

Graves, Robert & Pitarka, Arben. (2015). Refinements to the Graves and Pitarka (2010) Broadband Ground-Motion Simulation Method. Seismological Research Letters. 86. 10.1785/0220140101

Kishida, T., Ktenidou, O., Darragh, R.B., Silva, W.J. (2016). Semi-Automated Procedure for Windowing Time Series and Computing Fourier Amplitude Spectra for the NGA-West2 Database. PEER Report No. 2016/02, Pacific Earthquake Engineering Research Center, University of California, Berkeley, CA.

Konno, K. and Ohmachi, T., (1998). Ground-motion characteristics estimated from spectral ratio between horizontal and vertical components of microtremor, Bull. Seismol. Soc. Am. 88: 228−241. 58

Kottke A., Rathje E., Boore D.M., Thompson E., Hollenback J., Kuehn N., Goulet C.A., Abrahamson N.A., Bozorgnia Y., Der Kiureghian A., Silva W.J., Wang X. (2015). Selection of random vibration procedures for the NGA East Project, PEER report, in preparation.

Kutner, M., C. Nachtsheim, J. Neter, and W. Li (2005). Applied Linear Statistical Models,McGraw-Hill/Irwin, NewYork, NewYork, 1396 pp.

Magistrale, H., Day, S., Clayton, R.W. & Graves, R., 2000. The SCEC southern California reference three-dimensional seismic velocity model version 2, Bull. seism. Soc. Am., 90(6B), S65–S76.

Pacific Earthquake Engineering Research Center (PEER) (2015). NGA-East: Median ground-motion models for the Central and Eastern North America region, PEER Rept. No. 2014/05, Pacific Earthquake Engineering Research Center, University of California, Berkeley, California.

Small, P., D. Gill, P. J. Maechling, R. Taborda, S. Callaghan, T. H. Jordan, K. B. Olsen, G. P. Ely, and C. Goulet (2017). The SCEC unified community velocity model software framework, Seismological Research Letters 88(6), 1539–1552.

Taborda, R., S. Azizzadeh-Roodpish, N. Khoshnevis, and K. Cheng (2016). Evaluation of the southern California seismic velocity models through simulation of recorded events, Geophys. J. Int. 205, no. 3, 1342–1364, doi: 10.1093/gji/ggw085.

Villani, M. A., and N. Abrahamson (2015). Repeatable site and path effects on the ground-motion sigma based on empirical data from southern California and simulated waveforms from the CyberShake platform, Bull. Seismol. Soc. Am. 105, doi: 10.1785/0120140359.

Wang, F., and Jordan, T.H. (2014). Comparison of Probabilistic Seismic-Hazard Models Using Averaging-Based Factorization. Bulletin of the Seismological Society of America; 104 (3): 1230–1257. doi: https://doi.org/10.1785/0120130263

# 7. Appendix

Please follow this URL to download our CyberShake EAS flatfile:

https://drive.google.com/file/d/1hjoXOq2rqZst06kRXpOdx2l6LSmTxe7i/view?usp=sharing

Please follow this URL to access Scott Condon's tools for selection and acquisition of CyberShake simulations:

https://github.com/scndn/cybershake